Journal of Catalysis **191,** 138–146 (2000)
doi:10.1006/jcat.1999.2794, available online at http://www.idealibrary.com on IDEAL®

Adsorption and Photocatalytic Oxidation of Acetone on TiO_2: An *in Situ* Transmission FT-IR Study

M. El-Maazawi,*[,1] A. N. Finken,† A. B. Nair,† and V. H. Grassian†[,1]

**Department of Chemistry, United Arab Emirates University, Al-Ain, United Arab Emirates, and †Department of Chemistry, University of Iowa, Iowa City, Iowa 52242*

Received August 26, 1999; revised November 22, 1999; accepted December 13, 1999

In situ **transmission Fourier-transform infrared spectroscopy has been used to study the mechanistic details of adsorption and photocatalytic oxidation of acetone on TiO_2 surfaces at 298 K. The adsorption of acetone has been followed as a function of coverage on clean TiO_2 surfaces (dehydrated TiO_2). Infrared spectra at low acetone coverages ($\theta < 0.05$ ML) show absorption bands at 2973, 2931, 1702, 1448, and 1363 cm^{-1} which are assigned to the vibrational modes of molecularly adsorbed acetone. At higher coverages, the infrared spectra show that adsorbed acetone can undergo an Aldol condensation reaction followed by dehydration to yield $(CH_3)_2C{=}CHCOCH_3$, 4-methyl-3-penten-2-one or, more commonly called, mesityl oxide. The ratio of surface-bound mesityl oxide to acetone depends on surface coverage. At saturation coverage, nearly 60% of the adsorbed acetone has reacted to yield mesityl oxide on the surface. In contrast, on TiO_2 surfaces with preadsorbed water (hydrated TiO_2), very little mesityl oxide forms. Infrared spectroscopy was also used to monitor the photocatalytic oxidation of adsorbed acetone as a function of acetone coverage, oxygen pressure, and water adsorption. Based on the dependence of the rate of the reaction on oxygen pressure, acetone coverage, and water adsorption, it is proposed that there are potentially three mechanisms for the photooxidation of adsorbed acetone on TiO_2. In the absence of preadsorbed H_2O, one mechanism involves the formation of a reactive O^-(ads) species, from gas-phase O_2, which reacts with adsorbed acetone molecules. The second mechanism involves TiO_2 lattice oxygen. In the presence of adsorbed H_2O, reactive hydroxyl radicals are proposed to initiate the photooxidation of acetone.**

INTRODUCTION

Acetone represents a serious air pollutant for indoor environments, and its catalytic decomposition to less harmful compounds has been explored. Heterogeneous photocatalytic oxidation of acetone on TiO_2 (1–8), as well as other organic compounds (9–13), is one degradation method that has been the subject of several investigations. Peral and Ollis showed that acetone photooxidizes over TiO_2 in the presence of gas-phase O_2 to CO_2 and H_2O, and the initial rate of the reaction could be described by a Langmuir-Hinshelwood kinetic rate mechanism (1). No reaction intermediates were observed in those experiments. In contrast, Larson *et al*. reported that acetone may form a surface intermediate before complete oxidation (3).

The role of adsorbed water and lattice oxygen in photocatalytic oxidation reactions is unclear. Peral and Ollis reported that water vapor inhibited acetone oxidation (1). In other studies however, water, has been reported to enhance photocatalytic oxidation of other hydrocarbons such as formic acid over TiO_2 surface (14). Interestingly, it has also been shown that the photocatalytic oxidation of organics can occur without the presence of gas-phase molecular oxygen (3, 14). Although O_2 was found to be important for the complete oxidation of 2-propanol, Larson *et al*. observed that 2-propanol was photooxidized over TiO_2 even when no gaseous O_2 was present in the reactor (3). It was concluded that in the absence of gas-phase O_2 the photooxidation of propanol occurred via lattice oxygen atoms, and that gas-phase O_2 was needed only to replenish the produced oxygen vacancies. Muggli *et al*. studied the photocatalytic oxidation of acetic and formic acids by TiO_2 lattice oxygen (14–16). They determined that UV illumination was not necessary for gas-phase O_2 to replenish lattice oxygen vacancies. In the case of formic acid, they found that there were no differences in product formation for the oxidation of formic acid by lattice oxygen and oxidation by adsorbed O_2; however, they did observe a large increase in the initial rate of oxidation when gas-phase O_2 was present.

Herein we report on an *in situ* transmission FT-IR study of the adsorption and photocatalytic oxidation of acetone on TiO_2 at 298 K. FT-IR spectroscopy is a very effective technique for detecting both surface-bound and gas-phase intermediates in heterogeneous reactions. In the present study, *in situ* FT-IR spectroscopy is used to investigate the adsorption of acetone on TiO_2 and the formation of mesityl oxide as a function of acetone coverage and to characterize surface-bound and gas-phase products and intermediates formed in the photocatalytic oxidation reaction. At acetone

[1] Authors to whom correspondence should be addressed.

0021-9517/00 $35.00

coverages <0.1 ML, adsorbed acetone is photooxidized to gaseous CO_2 and H_2O on TiO_2. In the closed cell reactor used in this study, these gas-phase products can adsorb on TiO_2 to yield surface-bound CO_x and H_2O. At higher acetone coverages, near 0.5 ML, partial oxidation products are formed as well. In addition to characterizing products and intermediates in the photocatalytic reaction, the role of lattice and gas phase oxygen as well as absorbed water on the rate of acetone photocatalytic oxidation on TiO_2 was investigated. Based on the data presented here, several different mechanisms are proposed for acetone photocatalytic oxidation on TiO_2. The importance of each of these mechanisms depends on acetone coverage, oxygen pressure, and water coverage on the TiO_2 surface.

EXPERIMENTAL SECTION

Titania samples are made by spraying a slurry of the powdered TiO_2 (Degussa P25, surface area of $\sim$50 m^2/g) in deionized water ($\sim$4 g/100 ml) onto a tungsten grid, which is held at approximate 573 K. A template is used to mask half of the grid so that one side can be coated with TiO_2 powder, and the other side is left blank. Approximately 75 mg of the semiconductor powder is evenly coated onto a 3×1-cm area of the grid.

Once the grid is coated with the oxide, the grid is mounted inside the IR cell. The IR cell used in these experiments has been described previously (17). Briefly, the IR cell consists of a stainless-steel cube that is attached to a vacuum system consisting of an 80 L/s ion pump and 60 L/s turbo-molecular pump. After evacuation of the infrared cell to a pressures less than 10^{-6} Torr, the grid coated with the TiO_2 powder is then resistively heated to 673 K for 2 h under vacuum. The sample is then oxidized at the same temperature by introducing 100 Torr of oxygen into the IR cell for 30 min. After evacuating, the cell for 15 min, 100 Torr of oxygen is introduced into the cell, and the sample is let to cool to room temperature. Once the sample has reached room temperature, the cell is evacuated overnight. This cleaning procedure removes adsorbed hydrocarbon impurities, including carbonates, and adsorbed water from the surface. TiO_2 samples prepared this way are labeled as dehydrated TiO_2. An infrared spectrum of this surface (vide infra) shows the presence of isolated hydroxyl groups at frequencies of 3719 and 3672 cm^{-1}.

The IR cell is held in place by a linear translator inside the sample compartment of a Mattson RS-1 FT-IR spectrometer equipped with a narrowband MCT detector. The linear translator allows each half of the sample grid to be translated into the infrared beam. This permits the investigation of gas-phase and adsorbed species onto the photocatalyst surface under identical reaction conditions. Each spectrum was recorded by averaging 500 scans at an instrument resolution of 4 cm^{-1}. Each absorbance spectrum shown represents a single beam scan referenced to the appropriate single beam scan of the clean photocatalyst or the blank grid prior to gas introduction, unless otherwise noted.

A 500-W mercury lamp (Oriel Corp.) with a water filter was used as light source in these experiments. The 300-nm-long pass filter (with $\%T = 0$ at 300 nm) was placed in front of the lamp. The broadband light was then reflected off of a 1-in. quartz prism, and then turned by another 1-in. quartz prism onto the sample. The second quartz prism is mounted inside of the FT-IR sample compartment so that the dry air purge was not broken during irradiation. The power at the sample was measured before each experiment and was typically 180 mW/cm^2. The temperature of the sample did not exceed 315 K during these experiments.

Acetone (Aldrich, HPLC grade, 99+%) was transferred to a glass tube and subjected to several freeze-pump-thaw cycles before use. Oxygen (Air Products, 99.6%) was used as received. Double-deionized, ultrapure water was subjected to several freeze-pump-thaw cycles before being used in the hydrated surface experiments. Gas pressures were initially measured in a volume of 1159 ml and then expanded into the infrared cell, which is an additional 395 ml in volume. A valve between these two portions of the vacuum chamber was then closed before irradiation so that the reactants and products are contained inside the cell and can be monitored by IR spectroscopy.

For experiments with molecular oxygen present, acetone is allowed into the IR cell and allowed to equilibrate for 5 min. After that, 100 Torr of oxygen is introduced into the cell, and the valve to the cell is then closed and the mixture is left to equilibrate for 5 min before irradiation. In the preparation of the hydrated TiO_2 surface, 10 Torr of H_2O vapor is introduced into the cell then left to equilibrate for 15 min before evacuation.

RESULTS

Acetone Adsorption on TiO_2 as a Function of Pressure at 298 K

The infrared spectra of the clean TiO_2 surface (dehydrated TiO_2) as a function of increasing acetone pressure are shown in Fig. 1. The pressure (in mTorr) introduced into the IR cell (P_{in}) and the pressure measured after the system came to equilibrium (P_{eq}) are noted next to each spectrum shown in Fig. 1. Infrared spectra of the TiO_2 surface are referenced to the blank tungsten grid, and gas-phase contributions to the spectra shown in Fig. 1 have been subtracted out. Before the introduction of acetone into the infrared cell, only bands at 3719 and 3672 cm^{-1}, corresponding to isolated hydroxyl groups, are observed in the clean dehydrated TiO_2 spectrum. After acetone is introduced into the infrared cell at low pressures, there are new bands in the spectrum at 2973, 2931, 1702, 1422, 1366, and 1340 cm^{-1}.

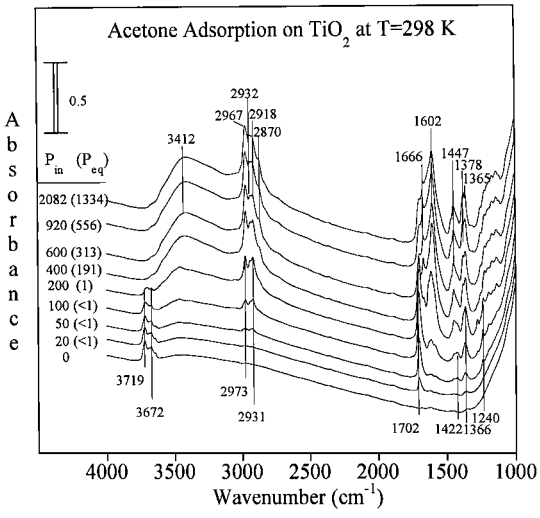

FIG. 1. Infrared spectra of acetone adsorbed on dehydrated TiO_2 at 298 K as a function of acetone pressure. The pressure introduced into the infrared cell (P_{in}) and the equilibrium pressure established in the infrared cell (P_{eq}) are given in units of mTorr. Absorptions assigned to adsorbed acetone are observed at 2973, 2931, 1702, 1422, 1366, and 1240 cm^{-1}. Absorptions assigned to adsorbed mesityl oxide are observed at 2967, 2932, 2918, 2870, 1666, 1602, 1447, 1378, and 1365 cm^{-1}. See text for further discussion.

These bands are assigned to adsorbed acetone on the TiO_2 particle surface. The assignment of the absorption bands due to molecularly adsorbed acetone is given in Table 1 (18). As the pressure of acetone increases, and therefore the coverage, the intensities of the bands due to adsorbed acetone initially increase and then decrease. In addition, several new bands in the spectra grow in as the acetone pressure is increased. These bands are observed at 3412, 2967, 2932, 2918, 2870, 1666, 1602, 1447, 1378, and 1365 cm^{-1} and can be assigned to adsorbed H_2O and mesityl oxide, the products of the acetone Aldol condensation reaction followed by dehydration,

$$2(CH_3)_2CO \rightarrow CH_3C(O)C{=}C(CH_3)_2 + H_2O. \quad [1]$$

The assignment of the absorption bands due to the hydrocarbon product of the acetone Aldol condensation/dehydration reaction, mesityl oxide, is also given in Table 1 (19, 20).

In order to quantify the amount of acetone adsorbed on the surface as a function of pressure, volumetric measurements of acetone into the infrared cell were made in the presence and absence of the TiO_2 sample. The difference in the pressure recorded after acetone is expanded into the infrared cell with and without the TiO_2 sample present is proportional to the number of molecules adsorbed on the TiO_2 powder. The number of adsorbed molecules per TiO_2 surface area can be calculated from the known volume of the system, the BET surface area of the TiO_2 powder, and the mass of the TiO_2 powder in the infrared cell. The amount of acetone that adsorbs from the gas phase as a function of the equilibrium pressure is plotted in Fig. 2. A fit to the data using a simple Langmuir adsorption model is also shown. Clearly this simple model does not accurately describe the adsorption process. The saturation coverage of acetone is determined to be 1×10^{15} molecules cm^{-2} at 298 K on TiO_2. This saturation coverage is defined as 1 monolayer (1 ML) of adsorbed acetone.

The infrared data show that there are two hydrocarbon species on the surface—acetone and mesityl oxide. Using the infrared data at very low acetone coverages, when acetone is present as the sole adsorbate on the surface TiO_2, combined with the volumetric measurements, the acetone extinction coefficient for the 1702 cm^{-1} band of adsorbed acetone can be calculated. From the infrared data, the estimated extinction coefficient of adsorbed acetone, and the volumetric measurements, the amounts of adsorbed acetone and mesityl oxide as a function of acetone coverage can then be determined. The results of this calculation are

TABLE 1

Vibration Assignment of Adsorbed Acetone and Mesityl Oxide Following Acetone Adsorption on Dehydrated TiO_2 at 298 K

Mode description	Frequency (cm^{-1})
Adsorbed acetone[a]	
ν(C–H)	2973, 2931
ν(C=O)	1702
$\delta_{as}(CH_3)$	1422
$\delta_s(CH_3)$	1366
ν(C–C)	1240
Adsorbed mesityl oxide[b]	
ν(C–H)	2967, 2932, 2918, 2870
ν(C=O)	1666
ν(C=C)	1602
$\delta_{as}(CH_3)$	1447
$\delta_s(CH_3)$	1378, 1365

[a] Assignment taken from Ref. (18).
[b] Assignment taken from Refs. (19, 20).

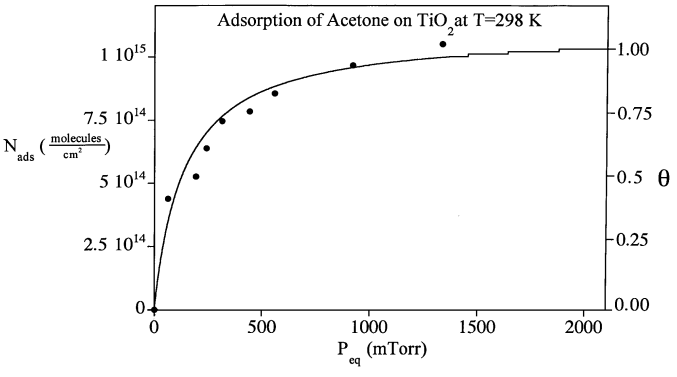

FIG. 2. The number of acetone molecules adsorbed on the TiO_2 surface at 298 K as a function of P_{eq} was determined from volumetric measurements. Saturation coverage of one monolayer is at 1×10^{15} molecules cm^{-2}.

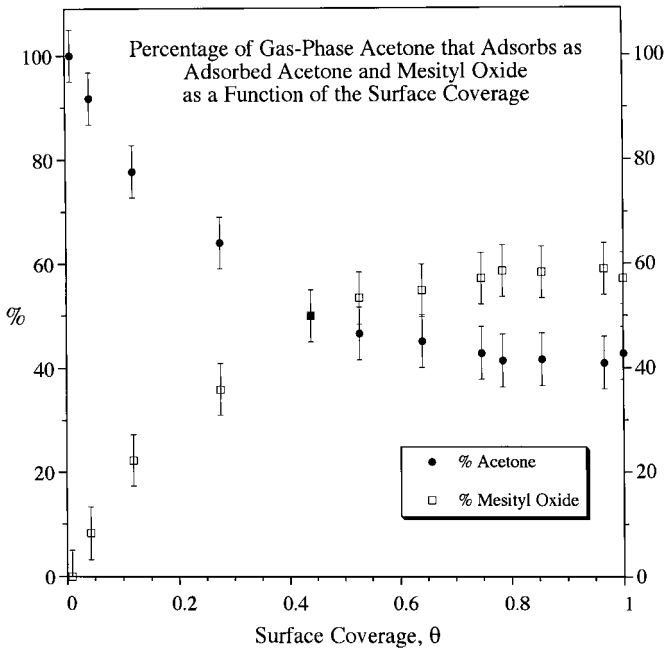

FIG. 3. The percentage of gas-phase acetone molecules that adsorb as acetone or mesityl oxide, the Aldol condensation product, has been calculated from the data presented in Figs. 1 and 2. See text for further discussion.

summarized in Fig. 3. Initially at low coverages, there is only adsorbed acetone on the surface but with increasing coverages the amount of mesityl oxide increases. At saturation coverage 60% of the acetone adsorbed from the gas phase is present as mesityl oxide on the surface while the remaining 40% is present as adsorbed acetone. The error in the percentages is estimated to be on the order of 5–10%.

Photocatalytic Oxidation of Acetone on Dehydrated and Hydrated TiO_2 in the Presence of Gas-Phase O_2

FT-IR spectroscopy was used to follow the photocatalytic oxidation of acetone on TiO_2. For these experiments, three acetone coverages were selected, $\theta = 0.01$, 0.10, and 0.50 ML. The lowest coverage of 0.01 ML of acetone was used in order to try and simulate indoor acetone concentrations, yet high enough to give good signal to noise ratio in the infrared experiments. At this coverage, only adsorbed acetone is present on the surface. The second coverage of 0.10 ML was chosen so as to investigate the effect of surface coverage on the photocatalytic oxidation of acetone. At this coverage, the predominant surface species is acetone; nearly 80% of the acetone adsorbed onto the surface is present in the molecular form. At the highest coverage investigated, 0.50 ML, 50% of the acetone that adsorbs on the surface reacts to give mesityl oxide and the other 50% adsorbed on the surface is present as molecular acetone. In addition to examining the role of acetone coverage on the photocatalytic oxidation process, the effect of adsorbed water is investigated by running experiments on two different TiO_2 surfaces—dehydrated and hydrated. As discussed under Experimental Section, TiO_2 samples that have been heated and calcined in oxygen and cooled down to room temperature contain little or no adsorbed water and are labeled as dehydrated TiO_2. TiO_2 samples that have been processed in the same way but then subsequently exposed to 10 Torr of water at room temperature are labeled as hydrated TiO_2.

Initially, to determine if there was a contribution from a thermal dark reaction, acetone reaction on TiO_2 at two coverages, 0.01 and 0.10 ML, was investigated. The sample was heated to 315 K in 100 Torr of oxygen in the absence of light. It was found that there were no changes in the infrared spectrum after following the reaction for nearly 200 min. However, there are marked changes in the infrared spectrum when $\lambda > 300$ nm light is used to irradiate the sample at 315 K. The infrared spectra following the photocatalytic oxidation of acetone on dehydrated TiO_2 in the presence of gas-phase oxygen (oxygen pressure = 100 Torr) at an acetone coverage of $\theta = 0.01$ ML as a function of irradiation time are shown in Fig. 4. The infrared spectra shown in this figure have been referenced to the clean dehydrated TiO_2 surface prior to adsorption of acetone. As can be seen in the spectra, as the photocatalytic oxidation of adsorbed acetone proceeds, infrared adsorption bands due to adsorbed product species are observed near 2957, 2873, 2358, 1575, 1441, 1358, and 1323 cm^{-1}. These bands are assigned to several species on the surface including adsorbed CO_2 and bidendate formate. The assignments of the bands due to the products formed following photocatalytic oxidation of acetone are given in Table 2 (21–23). The surface-bound

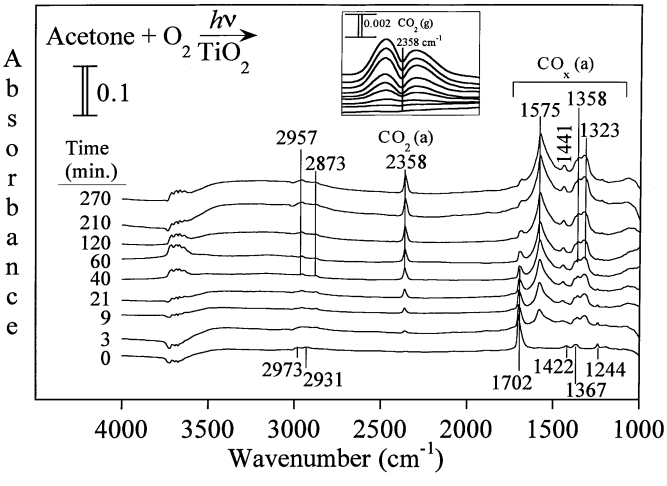

FIG. 4. Infrared spectra recorded as a function of irradiation time following the photooxidation of 0.01 ML of acetone on dehydrated TiO_2 at a gas-phase O_2 pressure of 100 Torr. Surface-bound species produced during photocatalytic oxidation of acetone are assigned to several adsorbed species. See Table 2 for an assignment of the photoproduct bands. The inset shows that gas-phase CO_2 is produced in these reactions.

TABLE 2

Vibration Assignment of Reaction Products from the Photocatalytic Oxidation of Acetone on Dehydrated TiO_2 at 298 K

Mode description[a]	Frequency (cm^{-1})
Adsorbed water	
ν(OH)	3324
δ(OH)	1641
Bidendate formate	
Combination band [ν_{as}(COO) + δ(CH)]	2957
ν_s(CH)	2873
ν_{as}(COO)	1575
ν_s(COO)	1358
δ(CH)	1323
Adsorbed carbon dioxide	
$\nu(CO_2)$	2358
Carbonate	
$\nu_s(CO_3^-)$	1441

[a] Assignments taken from Refs. (22, 23).

products are formed from the reaction of the gas-phase product CO_2 with the surface (21–23). The inset of Fig. 4 shows the gas-phase CO_2 product spectrum.

The infrared spectra following the photocatalytic oxidation of acetone on hydrated TiO_2 in the presence of gas-phase oxygen (oxygen pressure = 100 Torr) at an acetone coverage of $\theta = 0.01$ ML as a function of irradiation time are shown in Fig. 5. The infrared spectra shown in Fig. 5 are referenced to the clean hydrated TiO_2 surface prior to adsorption of either water or acetone. Prior to photocata lytic oxidation, absorption bands due to adsorbed acetone on the hydrated TiO_2 surface are seen in the bottom spectrum of Fig. 5. The band corresponding to ν(C=O) of acetone is shifted to a lower wavenumber of 1689 cm^{-1} on the hydrated surface. As the photocatalytic oxidation of adsorbed acetone proceeds, infrared absorption bands due to adsorbed photoproduct species grow in. The photoproduct bands are similar but shifted from those observed on the dehydrated sample. The photoproduct bands are assigned to primarily adsorbed bidendate formate and water. Interestingly, the band at 2358 cm^{-1}, corresponding to adsorbed CO_2, is not observed. This suggests that CO_2 does not adsorb as molecular CO_2 on the hydrated TiO_2 surface but instead desorbs into the gas phase. Gaseous CO_2 is in fact observed in the gas-phase infrared spectra following photocatalytic oxidation of acetone on the hydrated surface. As will be discussed, the amount of gas-phase CO_2 produced on the surface is greater on the hydrated surface compared to the dehydrated surface.

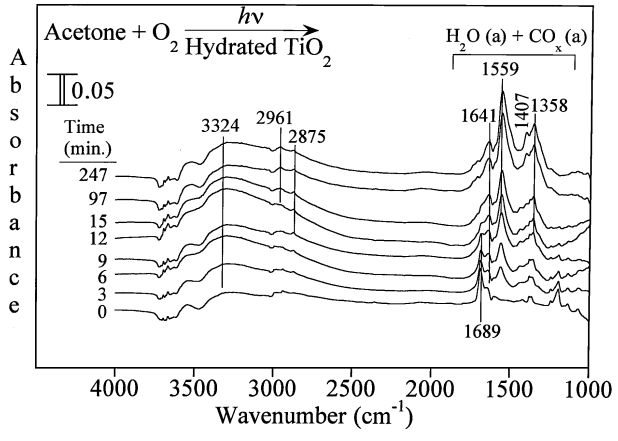

FIG. 5. Infrared spectra recorded as a function of irradiation time following the photooxidation of 0.01 ML of acetone on hydrated TiO_2 at a gas-phase O_2 pressure of 100 Torr. On the hydrated surface, the carbonyl stretching motion for adsorbed acetone shifts to lower frequency near 1689 cm^{-1}.

The infrared spectra (not shown) following the photocatalytic oxidation of acetone on hydrated and dehydrated TiO_2 in the presence of gas-phase oxygen (oxygen pressure = 100 Torr) at an acetone coverage of $\theta = 0.10$ ML as a function of irradiation time show similar product bands as the 0.01 ML data. Although product formation is similar for the photocatalytic oxidation of acetone on dehydrated TiO_2, the rate of photocatalytic oxidation of acetone is quite different.

The relative kinetic data for 0.01 and 0.10 ML acetone coverages on the dehydrated and the hydrated TiO_2 surfaces are shown in Fig. 6. Figure 6 displays a plot of the normalized integrated absorbance of the ν(C=O) band of adsorbed acetone, as a function of photolysis time. As can be seen in the figure, the rate of the photocatalytic oxidation of acetone in oxygen on hydrated TiO_2 is faster, at

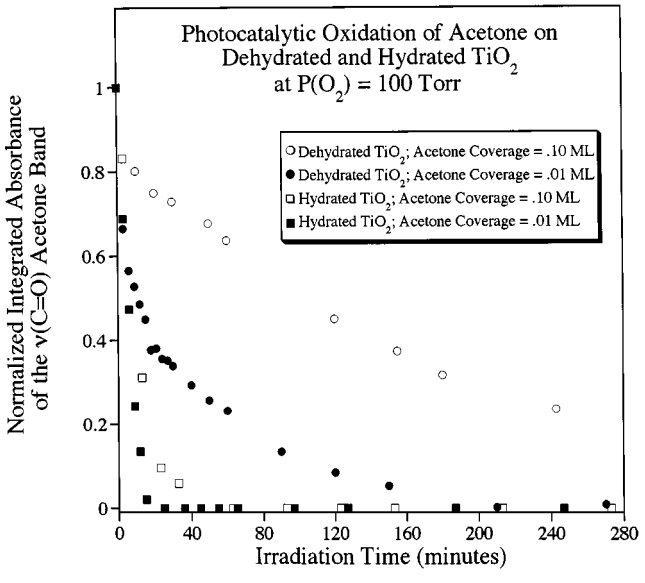

FIG. 6. Plot of the normalized integrated absorbance of the ν(C=O) band of adsorbed acetone following photooxidation of 0.01 and 0.1 ML of adsorbed acetone on both dehydrated and hydrated TiO_2 at a gas-phase O_2 pressure of 100 Torr.

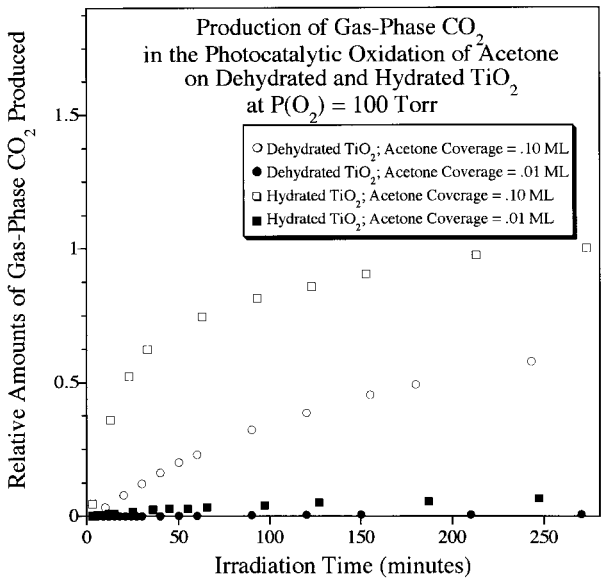

FIG. 7. Relative amounts of gas-phase CO_2 produced following the photooxidation of adsorbed acetone following photooxidation at two different coverages, 0.01 and 0.1 ML, on both dehydrated and hydrated TiO_2. The gas-phase O_2 pressure was 100 Torr in these experiments.

least for the coverage range from 0.01 to 0.1 ML, than on dehydrated TiO_2. The photocatalytic oxidation of acetone is complete in approximately 40 min regardless of the coverage on the hydrated surface. The initial rate of reaction on the hydrated TiO_2 surface is approximately 17 times higher than in the case of the dehydrated surface for $\theta = 0.01$, and even higher than that for $\theta = 0.10$. On the dehydrated surface, the photocatalytic oxidation of acetone is complete for 0.01 ML acetone coverage after 200 min of irradiation time. For an acetone coverage of 0.10 ML, there still remains 25% of the adsorbed acetone on the surface after 240 min of irradiation.

Comparisons between the production of gas-phase CO_2 during the photocatalytic oxidation of acetone on hydrated and dehydrated TiO_2 surfaces for both 0.01 and 0.10 acetone coverages are displayed in Fig. 7. The quantification of gas-phase CO_2 is obtained from a separate experiment where gas-phase CO_2 absorptions are calibrated as a function of pressure. More CO_2 is formed from the photocatalytic oxidation of acetone on the hydrated TiO_2 surface compared to the dehydrated TiO_2 surface. For the 0.10 ML coverage data, the initial rate of CO_2 production on the hydrated TiO_2 surface is nearly six times as great as it is on the dehydrated.

FT-IR analysis was also done for photocatalytic oxidation of acetone at even higher coverages, 0.5 ML, on hydrated and dehydrated TiO_2 samples. At this coverage on the dehydrated TiO_2 sample, 50% of the adsorbed acetone forms mesityl oxide on the surface and the other 50% is present as molecular acetone. The infrared data at high coverage show several differences from those of the low coverage. First, it shows that mesityl oxide does not photooxidize as readily as acetone. Second, it shows that another product is formed during photooxidation with absorptions near 1720 and 2840 cm^{-1}, which is assigned as a partial oxidation product, most likely formaldehyde. Similar experiments on the hydrated TiO_2 sample show that at 0.5 ML surface coverage there is much less mesityl oxide on the surface compared to adsorbed acetone. Approximately 70% of the acetone adsorbed on the surface is in the molecular form; the remaining 30% react on the surface to give mesityl oxide. Similar to the photocatalytic oxidation on dehydrated TiO_2, there is the formation of a partial oxidation product at this high coverage on the hydrated sample.

Photocatalytic Oxidation of Acetone on Dehydrated and Hydrated TiO_2 in the Absence of Gas-Phase O_2

The role of lattice oxygen and adsorbed water in the photocatalytic oxidation of acetone on TiO_2 was investigated by measuring the rate of acetone photocatalytic oxidation on both dehydrated and hydrated TiO_2 in the absence of gas-phase molecular oxygen. In these experiments, the TiO_2 sample was irradiated with light ($\lambda > 300$ nm) for two acetone coverages, 0.01 and 0.10 ML. As shown by FT-IR analysis, similar gas-phase and surface-bound products are seen in the absence of molecular O_2 as there were for when O_2 is present in the infrared cell. Plots of the normalized integrated absorbance of ν(C=O) band of adsorbed acetone versus irradiation time are shown in Fig. 8. At low coverages, 0.01 ML, a comparison between the initial rate of

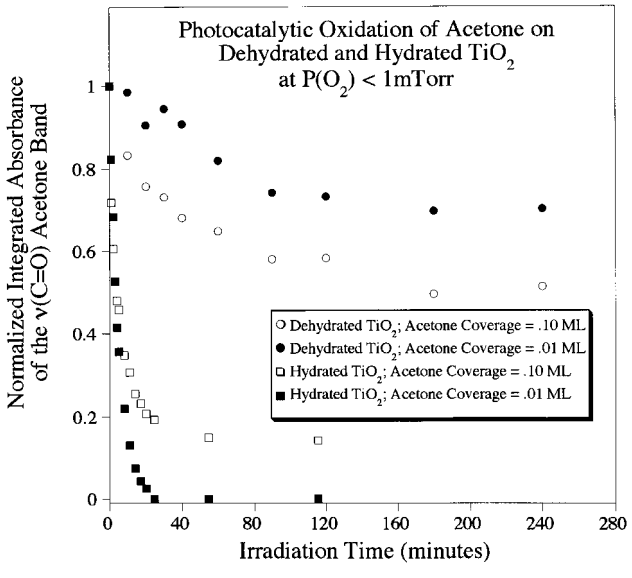

FIG. 8. Plot of the normalized integrated absorbance of the ν(C=O) band of adsorbed acetone following photooxidation of 0.01 and 0.1 ML of adsorbed acetone on both dehydrated and hydrated TiO_2 at a gas-phase O_2 pressure of <1 mTorr.

photocatalytic oxidation of acetone on dehydrated TiO_2 in the absence (Fig. 8) and in the presence gas-phase O_2 (Figure 6) shows that they are quite different. The initial rate of reaction when molecular oxygen is not present is far lower than the initial rate in the presence of gas-phase O_2. However, the initial rate of the reaction in the presence and absence of oxygen gas-phase O_2 at an acetone surface coverage of 0.10 M is the same. This indicates that the initial rate of the photooxidation process with lattice oxygen is acetone coverage dependent. The amount of acetone that photooxidizes after 240 min of irradiation in the absence of molecular oxygen is substantially less when there is no molecular oxygen, indicating that molecular oxygen is needed to sustain the photocatalytic oxidation process.

Very different results are seen for the photocatalytic oxidation of acetone at 0.01 and 0.10 ML coverages on hydrated TiO_2. There is very little difference in the rates of reaction for both coverages in the absence and presence of molecular oxygen on the hydrated TiO_2 surface. The main difference is that at 0.10 ML coverage, photocatalysis appears to turn off after 40 min and approximately 15% of adsorbed acetone remains on the surface in the absence of O_2. In the absence of molecular oxygen, all of the adsorbed acetone is photooxidized at a surface coverage of 0.01 ML on hydrated TiO_2.

DISCUSSION

Surface Reactions of Acetone on TiO_2

Acetone adsorption has been investigated on many surfaces including aluminum (224), silicon (24, 25), silica (26), silica-supported nickel (26), hematite (27), supported rhodium catalysts (28), NaCl (29), and titania (20, 24). On rutile TiO_2 surfaces, acetone was found to strongly adsorb onto Lewis acid sites followed by the formation of a surface enolate complex (20). The enolate surface complex can react further with another acetone molecule to yield mesityl oxide ($(CH_3)_2C{=}CHCOCH_3$). In this study, we were able to quantify the amount of mesityl oxide formed on the surface as a function of acetone pressure and showed that the amount of mesityl oxide that forms on the surface depends on the acetone coverage and the presence of water on the surface. At high surface coverages and in the absence of adsorbed water on the TiO_2 surface, mesityl oxide formation is favored. We have estimated that nearly 60% of acetone that adsorbs from the gas phase forms mesityl oxide on the surface. This means that at saturation coverage 3×10^{14} molecules/cm^{-2} of mesityl oxide are present on the surface and 4×10^{14} molecules/cm^{-2} of adsorbed acetone are present. However, when water is present on the surface much less mesityl oxide forms. Since water is a product of the Aldol condensation/dehydration reaction, the presence of adsorbed water will not favor the formation of mesityl oxide. In addition, water could adsorb on the active site for mesityl oxide formation. The assignment of the adsorption bands present in the infrared spectra following acetone adsorption is given in Table 1. This assignment is in agreement with others in the literature (19, 20). In addition, mesityl oxide product identification has been further confirmed by FT-IR spectroscopy by adsorbing mesityl oxide from the gas phase onto the TiO_2 surface.

Photocatalytic Oxidation of Acetone on TiO_2: The Role of Lattice Oxygen, Molecular O_2, and Adsorbed Water

At low coverages, it has been shown that in the presence of molecular oxygen and at acetone coverages of 0.01 and 0.10 ML, TiO_2 effectively mineralizes acetone to CO_2 and H_2O in agreement with earlier studies by Peral and Ollis (1). These products can adsorb on the TiO_2 surface to yield several different surface species. At higher coverages a partial oxidation product, identified as formaldehyde, forms on the surface, in agreement with earlier studies done at high coverage (30). Similar results were observed following the photooxidation of trichloroethylene on TiO_2; i.e., as the surface coverage increased and more trichloroethylene was photooxidized, surface sites were blocked for complete oxidation as partial oxidation products were formed and remove on the surface (15).

Several mechanisms have been postulated for the photoactivation of TiO_2 in the presence of molecular oxgyen. Oxygen is known to photoadsorb on TiO_2 via the reaction pathway shown below (31).

$$TiO_2 + h\nu \rightarrow h^+ + e^- \quad [2]$$

$$h^+ + e^- + OH^- \rightarrow OH + e^- \quad [3]$$

$$Ti^{4+} + e^- \rightarrow Ti^{3+} \quad [4]$$

$$O_2(ads) \rightarrow 2O(ads) \quad [5]$$

$$Ti^{3+} + O(ads) \rightarrow Ti^{4+} + O^-(ads). \quad [6]$$

The reactive species, O^-(ads), can further react with adsorbed acetone according to

$$(CH_3)_2CO(ads) + 8O^-(ads) \rightarrow\rightarrow\rightarrow 3CO_2(g) + 3H_2O(g), \quad [7]$$

where the multiple arrows mean that several steps are occurring in order to achieve complete oxidation. Gaseous CO_2 and H_2O can subsequently react with the surface to yield adsorbed products including adsorbed water and bidendate formate (22–24).

It is also evident that there is a significant contribution from TiO_2 lattice oxygen to the photocatalytic oxidation. Lattice oxygen effects are greater for higher coverages ($\theta = 0.10$ ML) than for lower ($\theta = 0.01$). The rate of photocatalytic oxidation of acetone at $\theta = 0.10$ ML is the same in the first 90 min in the presence and absence of O_2. This suggests that the lattice oxygen contribution to rate is significant at this coverage. At later times, the photoactive

lattice oxygen sites are depleted. The role of molecular oxygen then is to replenish these sites. The photooxidation of acetone by TiO_2 lattice oxygen is described by

$$(CH_3)_2CO(ads) + 8O(lattice) \rightarrow\rightarrow\rightarrow 3CO_2(ads) + 3H_2O(ads). \quad [8]$$

The large increase in the initial rate of reaction in gas-phase oxygen versus in the absence of lattice oxygen for $\theta = 0.01$ suggests that there are two different mechanisms involved in the photooxidation of acetone on TiO_2 at this coverage. The first mechanism which involves photoadsorption of gas-phase O_2 and the formation of adsorbed O^- which further reacts with adsorbed acetone. This is evident from Figs. 6 and 8. The second mechanism involves TiO_2 lattice oxygen. Photooxidation of acetone on TiO_2 by lattice oxygen is far slower than that by adsorbed O^- species at 0.01 ML coverage. These data suggest that as the acetone coverage increases the reaction with lattice oxygen becomes the predominant pathway.

On the hydrated surface, there is a large increase in the rate of the photocatalytic oxidation of acetone comapred to that on the dehydrated surface irrespective of the surface coverage and whether there is gas-phase O_2 present. Two possible mechanisms could explain these results. The first mechanism is that OH radicals on the hydrated surface are initiating the photocatalytic oxidation process. Similar to mechanisms proposed for the aqueous phase photooxidation of organics (11). The second mechanism is that hydroxyl radicals are effective traps for the holes, thus preventing electron-hole pair recombination. Therefore, the reduced titanium centers have longer lifetimes and more lattice oxygen atoms can be activated on the hydrated surface. Both mechanisms are consistent with the results presented here.

In other studies, water has been shown to inhibit acetone photooxidation on TiO_2 (1, 8). It has been suggested that a competitive adsorption between acetone and water is the cause of this inhibition. As the water pressure increases, there is an increase in the amount of adsorbed water and a decrease in the amount of acetone. This leads to a decrease in the rate of acetone photocatalytic oxidation. The amount of water used in the present study is lower than that used in the earlier studies as there is no overpressure of water. Furthermore, the amount of acetone that adsorbs, as indicated by the integrated area of the carbonyl stretch, is the same on the hydrated and dehydrated surfaces. Therefore, the competitive adsorption of acetone and water is not an issue under the experimental conditions used here. However at higher water pressures, this will indeed be the case.

CONCLUSION

The data presented here show that the formation of mesityl oxide during the adsorption of acetone on TiO_2 is a function of acetone coverage and preadsorbed water on the surface of the TiO_2 sample. Acetone adsorbs predominantly in the molecular form at low coverages ($\theta <$ 0.01 ML); the amount of mesityl oxide that forms increases as a function of acetone coverage. At low acetone coverages, (<0.10 ML) acetone is oxidized predominantly to gaseous CO_2 and H_2O, on both hydrated and dehydrated TiO_2 surfaces, irrespective of the coverage. These gas-phase products can adsorb onto the surface. At larger acetone coverages, formaldehyde is also observed in the FT-IR spectrum. The rate of the photocatalytic oxidation reaction is higher on the TiO_2 hydrated surface than that on the dehydrated TiO_2 surface. Under the various conditions used in these studies, there may be potentially three different photocatalytic oxidation mechanisms. The rate-determining step in one mechanism is the formation of the reactive species O^-(ads) from gas-phase O_2. A second mechanism involves photooxidation of TiO_2 lattice oxygen. A third mechanism involves hydroxy radical reactions on the hydrated TiO_2 surface, similar to aqueous-phase photooxidation mechanisms.

ACKNOWLEDGMENTS

The authors gratefully acknowledge the NSF (Grant CHE-9614134) and DOE (Grant DE-FG01-98ER62580) for support of this work.

REFERENCES

1. Peral, J., and Ollis, D. F., *J. Catal.* **136**, 554 (1992).
2. Lichtin, N. N., Avudaithai, M., Berman, E., and Dong, J., *Res. Chem. Intermed.* **20**, 755 (1994).
3. Larson, S. A., Widegren, J. A., and Falconer, J. L., *J. Catal.* **157**, 611 (1995).
4. Alberici, R. M., and Jardim, W. F., *J. Adv. Oxid. Technol.* **3**, 182 (1998).
5. Alberici, R. M., and Jardim, W. F., *Appl. Catal. B* **14**, 55 (1997).
6. Stevens, L., Lanning, J. A., Anderson, L. G., Jacoby, W., and Chornet, N., *J. Air Waste Manag. Assoc.* **48**, 979 (1998).
7. Vorontsov, A. V., Barannik, G. B., Snegurenko, O. I., Savinov, E. N., and Parmon, V. N., *Kinet. Catal.* **38**, 97 (1997).
8. Sauer, M. L., and Ollis, D. F., *J. Catalysis* **149**, 81 (1994).
9. Matthews, R. W., *J. Catal.* **111**, 264 (1988).
10. Hoffmann, M. R., Martin, S. T., Choi, W., and Bahnemann, D. W., *Chem. Rev.* **95**, 69 (1995).
11. Fox, M. A., and Dulay, M. T., *Chem. Rev.* **93**, 341 (1993).
12. Blake, D. M., National Renewable Energy Laboratory Technical Report No. 570-26797, 1999.
13. Linsebigler, A. L., Lu, Guangquan, and Yates, J. T., Jr., *Chem. Rev.* **95**, 735 (1995).
14. Muggli, D. S., Keyser, S. A., and Falconer, J. L., *Catal. Lett.* **55**, 129 (1998).
15. Muggli, D. S., and Falconer, J. L., *J. Catal.* **186**, 230 (1999).
16. Muggli, D. S., and Falconer, J. L., *J. Catal.*, in press.
17. Driessen, M. D., Goodman, A. C., Miller, T. M., Zaharias, G. A., and Grassian, V. H., *J. Phys. Chem. B* **102**, 549 (1998).
18. Shimanouchi, T., Tables of Molecular Vibrational Frequencies, Vol. 1, National Standard Reference Data Series, NBS (US), 1972.
19. Panov, A. G., and Fripiat, J. J., *Langmuir* **14**, 3788 (1998).
20. Griffiths, D. M., and Rochester, C., *J. Chem. Soc. Faraday Trans. I* **74**, 403 (1978).

21. Goodman, A., and Grassian, V. H., unpublished results.
22. Driessen, M. D., and Grassian, V. H., *J. Phys. Chem*. **99**, 16519 (1995).
23. Bando, K. K., Sayama, K., Kusama, H., Okabe, K., and Arakawa, H., *Appl. Catal. A* **165**, 391 (1997).
24. Kiselev, A. V., and Uvarov, A. V., *Surf. Sci.* **6**, 399 (1967).
25. Allian, M., Borello, E., Ugliengo, P., Spano, G., and Garrone, E., *Langmuir* **11**, 4811 (1995).
26. Young, R. P., and Sheppard, N., *J. Catal.* **7**, 223 (1967).
27. Busca, G., and Lorenzelli, V., *J. Chem. Soc. Faraday Trans. I* **78**, 2911 (1982).
28. Dai, C. H., and Worley, S. D., *Langmuir* **4**, 326 (1988).
29. Richardson, H. H., *J. Phys. Chem*. **96**, 5898 (1992).
30. Bickley, R. I., Munuera, G., and Stone, F. S., *J. Catal.* **31**, 389 (1973).
31. Munuera, G., Rives-Arnau, V., and Saucedo, A., *J. Chem. Soc. Faraday Trans. I* **78**, 736 (1979).